Escola de Primavera de Transição e Turbulência
Blumenau 2020

ABCM Associação Brasileira de Engenharia e Ciências Mecânicas

12th Spring School on Transition and Turbulence
September 21st-25th, 2020, Blumenau, SC, Brazil

EPTT-2020-0025
EVALUATION OF THE ACCURACY OF THERMAL RADIATION MODELS IN THE ABSENCE AND PRESENCE OF TURBULENT FLUCTUATIONS

Bruno de Luca Zimmer Gomes
Guilherme Crivelli Fraga
Francis Henrique Ramos França
Universidade Federal do Rio Grande do Sul, Department of Mechanical Engineering – Rua Sarmento Leite, 425, Porto Alegre, Brazil
bruno.luca@ufrgs.br; guilhermecfraga@ufrgs.br; frfranca@ufrgs.br

Abstract. *Radiation is often the main heat transfer mechanism for problems that involve high temperatures such as reactive flows, where the presence of species such as H_2O and CO_2, produced in the combustion process. This paper analyzes the accuracy of spectral models in the presence or absence of turbulent fluctuations. Fluctuations of the medium properties are known to affect the radiation field, in a phenomenon that is named turbulence-radiation interaction (TRI), which originates from the highly non-linear coupling between fluctuations of the radiation intensity and fluctuations of temperature and medium composition. The accuracy of different formulations of the weighted-sum-of-gray-gases model, are compared with a reference solution given by line-by-line integration of the radiative transfer equation. The test cases consists of a line-of-sight calculations based on scalar fields obtained experimentally for the Sandia flame D. The mean total radiation intensity $\overline{I}$ along the line-of-sight is computed considering and neglecting turbulent fluctuations of temperature. Results show that the fluctuations substantially increase $\overline{I}$ for both solutions and the average errors associated to the WSGG model are of approximately* 9 % *considering turbulent fluctuations; when disregarding fluctuations, this error in general increases, although only slightly.*

Keywords: *turbulence-radiation-interaction, thermal radiation, temperature fluctuations, spectral models, Sandia flame D.*

1. INTRODUCTION

Among other factors, turbulence is characterized by a high level of irregularity, so it is often not possible to carry out a deterministic analysis of the phenomenon. Therefore, a statistical treatment is usually necessary to solve problems involving turbulence, through the usage of modeling approaches such as Reynolds-Averaged Navier-Stokes (RANS) and Large Eddy Simulation (LES) (Pope, 2000; Wilcox, 2006). On the other hand, thermal radiation is the main heat transfer mechanism for problems involving high temperatures, as in reactive flows; for these configurations, the presence of species such as H_2O and CO_2, produced in the combustion process, further enhance the radiative transfer, for they participate in the radiation exchange (Howell *et al.*, 2016; Modest and Haworth, 2016).

The interaction between these two processes (i.e., turbulence and radiation, in what is referred to as turbulence-radiation interaction, or TRI) is an additionally complex phenomenon, due to the highly non-linear coupling between fluctuations of the radiation intensity and fluctuations of temperature and medium composition. In particular for reacting flows, neglecting these fluctuations when solving the radiation field can lead to large errors—that is, mean radiative quantities may significantly differ from these quantities computed from the mean temperature and mean species concentrations. The importance of adequately considering TRI has been demonstrated numerically, theoretically and experimentally for a number of different types of combustion configurations (Coelho, 2007).

One of the central challenges when modeling the radiative exchange in participating media is capturing the how the radiative properties vary with the radiation spectrum. For this purpose, many spectral models have been developed, with different levels of complexity, computational cost and accuracy. However, because turbulence is known to affect distinct regions of the radiation spectrum in different manners (Hall and Vranos, 1994), it is possible that the performance of any given spectral model not be the same when evaluated for media in the presence or not of turbulent fluctuations. Nevertheless, as far as the authors' know, there has not been much effort in including TRI effects in the assessment of the accuracy of spectral models.

The exception to that is the set of studies made by Krishnamoorthy and collaborators (Krishnamoorthy, 2012, 2010; Krishnamoorthy *et al.*, 2005b,a), which attempted to incorporate the effect of turbulent fluctuations in the evaluation of non-gray and gray gas radiation models. In those studies, only TRI effects on the radiative emission were considered, and

were modeled through the simple approximation developed by Snegirev, 2004, which determines the mean emission in terms of the mean temperature, mean species concentrations and temperature variance. Absorption TRI was neglected and the mean radiative absorption was determined by invoking the optically thin fluctuation approximation, OTFA (Kabashnikov and Kmit, 1979). Experimental data for temperature, medium composition and temperature variance were used to feed the calculations, and the results for radiative quantities were compared either to measurements or to other spectral models. Of particular intereset to the present text is the study reported in Krishnamoorthy, 2010, where the accuracy of different formulations of the weighted-sum-of-gray-gases (WSGG) model was assessed for the Sandia flame D by comparisons with the spectral line-based WSGG (SLW) model including the effect of turbulent fluctuations, with mostly positive results.

The present paper carries out a similar analysis, but with more emphasis given to the effect of the strength of turbulence fluctuations on the accuracy of the WSGG model. This is done by solving the radiative transfer problem along specific paths for the same mean temperature and mean medium composition fields (extracted from experimental measurements) while neglecting turbulent fluctuations and considering them with different levels of turbulence intensity. Furthermore, instead of the SLW model, the line-by-line integration approach is used as the reference for the comparisons, which provides the most accurate representation available of the spectral behavior of the gas radiative properties.

2. METHODOLOGY

2.1 Thermal radiation in participating media

The variation of spectral radiation intensity I_η along the path s is described by the radiative transfer equation (RTE), which, for a non-scattering medium, is given as (Modest, 2013)

$$\frac{\mathrm{d}I_\eta}{\mathrm{d}s} = -\kappa_\eta I_\eta + \kappa_\eta I_{b\eta}\,, \tag{1}$$

where $I_{b\eta}$ is the spectral blackbody radiation intensity or Planck function, κ_η is the spectral absorption coefficient, and η denotes the dependence on the radiation spectrum. Note that the first term on the right-hand side of this equation represents the absorption of radiation along ds, whereas the second term corresponds to the local emission of radiation.

For future discussion, it is useful to also present the spectrally-integrated form of Eq. (1), that is given as

$$\frac{\mathrm{d}I}{\mathrm{d}s} = -\kappa_G I + \kappa_P I_b\,. \tag{2}$$

In this equation, I_b is the total blackbody intensity ($I_b = \int_0^\infty I_{b\eta}\,\mathrm{d}\eta$), and κ_G and κ_P are the incident-mean and Planck-mean absorption coefficients. To ensure the consistency of the formulation, these two quantities are expressed as $\kappa_G = \int_0^\infty \kappa_\eta I_\eta\,\mathrm{d}\eta\,/I$ and $\kappa_P = \int_0^\infty \kappa_\eta I_{b\eta}\,\mathrm{d}\eta\,/I_b$.

2.2 Line-by-line (LBL) integration

If the dependence of κ_η of the wavenumber η in Eq. (1) is known, then that equation can be solved for each spectral position and the resulting I_η be integrated over the whole spectrum to obtain the total intensity I, $I = \int_0^\infty I_\eta\,\mathrm{d}\eta$. This is the line-by-line integration method, and it usually relies on a high-resolution spectral database, such as the HITRAN (Rothman *et al.*, 2013) or HITEMP (Rothman *et al.*, 2010) databases, for determining the spectral absorption coefficient.

In this paper, the HITEMP 2010 database is used for this purpose. The absorption spectra of H_2O and CO_2 (the only species considered to participate in the radiative transfer process for the present calculations) are extracted at a 150 000 spectral intervals between $\eta = 0\,\mathrm{cm}^{-1}$ and $\eta = 10^4\,\mathrm{cm}^{-1}$, yielding a spectral resolution of $0.067\,\mathrm{cm}^{-1}$. Spectral line broadening is described by the Lorentz profile, adopting a line-wing cutoff of $40\,\mathrm{cm}^{-1}$ for water vapor H_2O and $800\,\mathrm{cm}^{-1}$ for carbon dioxide. For H_2O, the absorption spectra are constructed at partial pressures of 0.01 atm, 0.1 atm, 0.2 atm and 0.4 atm (the total pressure is always set to 1.0 atm), with linear interpolation adopted for intermediary partial pressures; for CO_2, since it does not present a significant self-broadening effect Howell *et al.* (2016), the spectrum for any partial pressure is determined by linearly interpolating data produced for 0.1 atm. For temperature, the spectral data are generated for temperatures between 400 K and 2400 K, in intervals of 100 K, and linear interpolation is again adopted for intermediary temperatures. More information on the procedure of obtaining the H_2O and CO_2 absorption lines is given in Dorigon *et al.*, 2013; Cassol *et al.*, 2014.

2.3 The weighted-sum-gray-gases (WSGG) model

The WSGG model replaces the complex absorption spectrum of a participating medium as a small set of J gray gases with constant absorption coefficient that occupy non-contiguous spectral intervals, and transparent windows with null absorption coefficient. Based on this representation, the integration of Eq. (1) across the spectral interval corresponding to

a single gray gas results in (Modest, 1991)

$$\frac{\mathrm{d}I_j}{\mathrm{d}s} = -\kappa_j I_j + \kappa_j a_j I_b \,, \tag{3}$$

where I_j is the partial intensity of gas j, κ_j is its absorption coefficient, and a_j its emission weighting coefficient, which represents the fraction of blackbody energy that lies within the spectral interval corresponding to gas j. Once Eq. (3) is solved for all J gases, as well as for the transparent windows (which are conventionally denoted by the index $j = 0$), the total intensity is determined as $I = \sum_{j=0}^{J} I_j$.

The dependence of κ_j and a_j on the local thermodynamic state of the medium is typically determined by fitting the total emittance to some reference data (often, the emittance determined by LBL integration of a high-resolution spectral database). Several WSGG formulations, differing on how this dependence is expressed, have been developed so far, usually applicable to a specific range of applications (e.g., air-fuel combustion at atmospheric conditions, oxy-fuel combustion, sooting flames). Here, some of the most widely used and contemporaneous WSGG approaches are considered: the formulation of Dorigon *et al.*, 2013, applicable to methane-air combustion; the superposition methodology proposed by Cassol *et al.*, 2014; the model by Yin, 2013, that encompasses many different products of air-fuel combustion; and the formulation of Kangwanpongpan *et al.*, 2012, that was originally developed for oxy-fuel combustion.

2.4 Turbulence-radiation interaction (TRI)

As previously noted, TRI arises from the highly non-linear coupling between fluctuations of the temperature and medium composition and fluctuations of the radiation intensity. To illustrate this, consider the time-averaging of Eq. (1), that leads to

$$\frac{\mathrm{d}\overline{I_\eta}}{\mathrm{d}s} = -\overline{\kappa_\eta I_\eta} + \overline{\kappa_\eta I_{b\eta}} \,, \tag{4}$$

where the overbar denotes the time-averaging operation. In the presence of turbulent fluctuations, the correlations that appear on the right-hand side of this equation often cannot be neglected—i.e., $\overline{\kappa_\eta I_\eta} \neq \overline{\kappa_\eta}\,\overline{I_\eta}$ and $\overline{\kappa_\eta I_{b\eta}} \neq \overline{\kappa_\eta}\,\overline{I_{b\eta}}$. Moreover, the values of both $\overline{\kappa_\eta}$ and $\overline{I_{b\eta}}$ may differ significantly from these quantities evaluated at the mean temperature and mean medium composition. These two factors combined explain the large errors that occur when the mean radiation field is solved on the basis of mean quantities only, as it is common in RANS simulations of turbulent combustion. Comprehensive reviews on the state-of-the-art of TRI studies and modeling are reported in Coelho, 2007, and Modest and Haworth, 2016.

To capture the TRI effects, this paper invokes the OTFA for modeling $\overline{\kappa_\eta I_\eta}$. This approximation simplifies the mean absorption term by neglecting the cross-correlation between the absorption coefficient and the local intensity, yielding $\overline{\kappa_\eta I_\eta} = \overline{\kappa_\eta}\,\overline{I_\eta}$, which greatly reduces the complexity of the problem. The validity of such approximation has been verified for a number of non-sooting turbulent flames, including the Sandia flame D (Coelho, 2012; Gupta *et al.*, 2013). Conversely, for the emission term, the model developed by Snegirev, 2004, is adopted, originally introduced for approximating the mean total emission and given as

$$\overline{\kappa_P I_b} = \overline{\kappa_P} I_b(\overline{T}) \left(1 + 6 C_{TRI,1} \frac{\overline{T'^2}}{\overline{T}^2} + 4 C_{TRI,2} \frac{\overline{T'^2}}{\overline{\kappa_P}\,\overline{T}} \left.\frac{\partial \kappa_P}{\partial T}\right|_{\overline{T}} \right), \tag{5}$$

where $I_b(\overline{T})$ is the total emission evaluated at the local mean temperature, and $C_{TRI,1}$ and $C_{TRI,2}$ are the constants of the model. As it was done in many previous applications of Snegirev's model—as in the series of studies by Krishnamoorthy and collaborators (Krishnamoorthy, 2012, 2010; Krishnamoorthy *et al.*, 2005b,a)—the last term of Eq. (5) is neglected by setting $C_{TRI,2} = 0$, in which case the model can be straightforwardly applied for approximating $\overline{\kappa_\eta I_{b\eta}}$,

$$\overline{\kappa_\eta I_{b\eta}} = \overline{\kappa_\eta} I_{b\eta}(\overline{T}) \underbrace{\left(1 + 6 C_{TRI,1} \frac{\overline{T'^2}}{\overline{T}^2} \right)}_{\beta}, \tag{6}$$

where $I_{b\eta}(\overline{T})$ is the Planck function evaluated at the mean temperature. By denoting the term within parenthesis in the above equation as an emission-TRI correction factor β, the final form of the time-averaged RTE solved in this study is reached:

$$\frac{\mathrm{d}\overline{I_\eta}}{\mathrm{d}s} = -\overline{\kappa_\eta}\,\overline{I_\eta} + \beta \overline{\kappa_\eta} I_{b\eta}(\overline{T}) \,. \tag{7}$$

The time-averaged form of the RTE in the framework of the WSGG model is obtained by time-averaging Eq. (3),

$$\frac{\mathrm{d}\overline{I_j}}{\mathrm{d}s} = -\overline{\kappa_j I_j} + \overline{\kappa_j a_j I_b} \,, \tag{8}$$

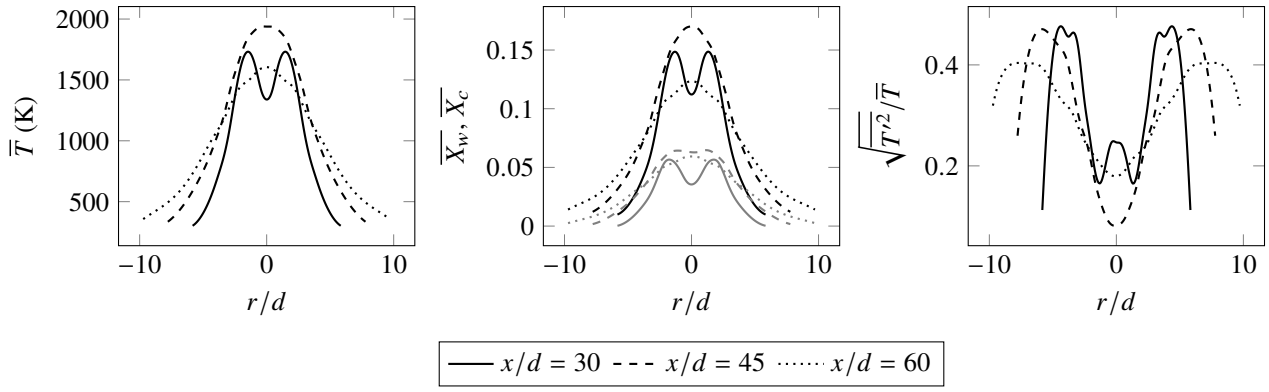

Figure 1. Mean temperature, mean CO_2 and H_2O mole fractions (in black and gray, respectively), and temperature fluctuation intensity at the three radial lines considered for the calculations in this study

Following similar modeling approaches as those adopted for Eq. (4), the above equation becomes

$$\frac{\mathrm{d}\overline{I_j}}{\mathrm{d}s} = -\overline{\kappa_j}\overline{I_j} + \beta\overline{\kappa_j} a_j(\overline{T}) I_b(\overline{T}) \,, \tag{9}$$

with $a_j(\overline{T})$ the weighting coefficient evaluated at the mean temperature. For $\overline{\kappa_j}$, as well as for $\overline{\kappa_\eta}$ in Eq. (7), the value of the quantity evaluated at the mean temperature and mean medium composition is used for the present calculations.

3. CONFIGURATION UNDER STUDY

The radiative transfer calculations are carried out for three optical paths based on experimental data obtained for the Sandia flame D. This is a very well-documented flame (Barlow and Frank, 1998), consisting of a fuel jet with a mixture of 25 % methane and 75 % air (in volume), that is accompanied by an annular pilot flow (a burnt CH_4-air mixture with equivalence ratio of 0.7), which in turn is surrounded by an outer coflow of air. The fuel jet has a diameter $d = 7.2$ mm and a Reynolds number of 22 400. Previous studies have already shown that TRI effects can be significant for this flame (Coelho *et al.*, 2003; Coelho, 2004; Gupta *et al.*, 2013).

The three optical paths considered here corresponds to radial lines at different heights x above the jet inlet: $x/d = 30$, $x/d = 45$ and $x/d = 60$. The value of the mean temperature, mean species concentrations of CO_2 and H_2O ($\overline{X_c}$ and $\overline{X_w}$, respectively), and temperature fluctuation intensity ($\sqrt{\overline{T'^2}}/\overline{T}$, necessary for computing the correction factor β, cf. Eq. (6)) along these lines are extracted from the data available at the TNF workshop website (TNF, 2020), and are depicted in Fig. 1. Because the scalar data is only available for approximately fifteen spatial points, cubic splines were used to obtained values for all grid points in the numerical solution

4. RESULTS

The time-averaged RTE, Eqs. (7) and (9), is numerically integrated along the three optical paths mentioned in Chapter 3. A total of 100 uniformly distributed integration points are used for this purpose; results obtained with this number of points were found to differ by at most 0.32 % from those attained by adopting 200 integration points. As a boundary condition, the intensity at the beginning of the optical is taken as a blackbody evaluated at the local temperature, where in it's formulation the emission term multiplied by the Stefan-Boltzmann constant and the temperature is elevated in the fourth power. For the LBL method, Eq. (4) is solved with κ_η computed following the methodology described in Section 2.2for the WSGG model, the formulations of Cassol *et al.*, 2014, Dorigon *et al.*, 2013, Yin, 2013, and Kangwanpongpan *et al.*, 2012 are tested (for conciseness, these formulations will be referred next as C. *et al.*, D. *et al.*, K. *et al.*, and Yin, respectively). In both cases, the mean radiation intensity is computed considering turbulent fluctuations—using data for the temperature fluctuation intensity to calculate the emission-TRI correction factor β—and neglecting them by setting $\beta = 1$.

4.1 Comparison between models in the absence and presence of TRI

Figure 2 depicts the results for the mean total radiation intensity $\overline{I}$ for the three optical paths ($x/d = 30$, 45 and 60) as calculated by the each WSGG formulation and by the benchmark LBL method considering and neglecting turbulent fluctuations ("TRI" and "No-TRI", respectively). Including scalar fluctuations in the RTE solution field has a clear effect on the mean radiation field, resulting in an approximate average increase of 70 % in $\overline{I}$. This occurs because the TRI correction

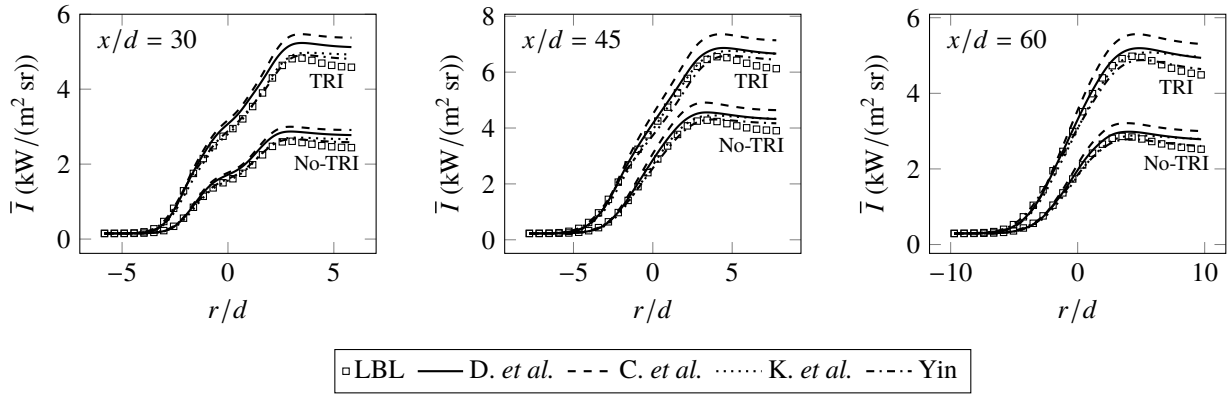

Figure 2. Mean radiation intensity predicted considering and neglecting turbulent fluctuations ("TRI" and "No-TRI") by each WSGG formulation and by the benchmark LBL method.

factor β is greater than unity for the entire optical path (because the temperature variance $\overline{T'^2}$ is always positive, see Eq. (6)), so the "TRI" solutions will predict a larger radiation emission than the "no-TRI" ones.

Overall, the WSGG model is capable of a fairly good estimate of the mean radiation intensity. The most accurate results are provided by the formulation of Yin, 2013, followed by the one by Kangwanpongpan *et al.*, 2012, with the worst results obtained by the superposition method of Cassol *et al.*, 2014. It should be noted that some WSGG formulations that allow for a varying H_2O/CO_2 mole fraction ratio were also tested, such as the one by Bordbar *et al.*, 2014, but they led to unphysical results due to the fact that this ratio may be exceedingly large at the start or at the end of the optical path; therefore, the results of these formulations are not included here.

Whether turbulent fluctuations are considered or not does not appear to influence the accuracy of any of the WSGG formulations. For instance, the average error for the model of Yin *et al.*, 2010, in the calculation of the mean radiation intensity along the $x/d = 30$ line is about 1.7 % for the "no-TRI" solution and reduces to 1.0 % for the "TRI" one (cf. Table 1); for the $x/d = 60$ line, the error increases from 1.4 % to 1.7 % when turbulent fluctuations are included. The issue of how the accuracy of the WSGG model is influenced by different levels of turbulence is investigated next.

4.2 Comparison of models for different TRI levels

Two additional radiative transfer calculations have also been carried out, where the intensity of temperature fluctuations is scaled down or up by 50 % from what is shown in Fig. 1. This is done with the purpose of better understanding how turbulent fluctuations affect the accuracy of the WSGG model.

A local normalized error of each WSGG formulation may be defined as $\Delta = |\overline{I}_{\mathrm{LBL}} - \overline{I}_{\mathrm{WSGG}}| / \max(\overline{I}_{\mathrm{LBL}})$, where $\overline{I}_{\mathrm{LBL}}$ and $\overline{I}_{\mathrm{WSGG}}$ are the local mean intensities obtained by the LBL method and the WSGG model, respectively, and $\max(\overline{I}_{\mathrm{LBL}})$ is the maximum local value of $\overline{I}_{\mathrm{LBL}}$. From this definition, Table 1 reports the maximum Δ (Δ_{max}) and the path-averaged Δ (Δ_{avg}) for each WSGG formulation at each one of the three optical paths, and for the four turbulence intensities TI considered. The results for $TI = 0$ % and $TI = 100$ % correspond to those of the "No-TRI" and "TRI" solution discussed in Section 4.1

In general, turbulent fluctuations lead to a decrease in both Δ_{max} and Δ_{avg}, indicating that TRI may contribute to improving the performance of the WSGG model. However, this is not always the case—for instance, as already noted, the errors of the formulation of Yin, 2013 tend to increase with the introduction of turbulent fluctuations for $x/d = 60$. Table 1 also better illustrate how this formulation performs the best among the ones tested in this paper; its average error never surpasses 2.2 %, and the maximum error is never above 6.2 %. Conversely, the formulation of Cassol *et al.*, 2014 presents the larger errors, with Δ_{max} reaching upwards of 18.0 %.

Figures 3–6 report the mean intensity calculated by each WSGG formulations for each turbulence intensity alongside with the profile of the error Δ. The results of the LBL method are also included for reference. The same trends of Fig. 2 can be observed in this figure—i.e., throughout the optical path, $\overline{I}$ is increased with increasing TI. With the exception of K. *et al.* at the start of the optical path, all WSGG formulations tend to overestimate the mean intensity.

It is interesting to note that, for all but Yin's WSGG formulation, there is a clear divide in the optical path: up to a particular value of r/d, increasing the intensity of turbulent fluctuations increases the error of the model, and afterwards, this behavior is inverted. This inversion occurs at the same position for the formulations of Dorigon *et al.*, 2013, and Cassol *et al.*, 2014, but it happens farther on along the optical path for the formulation of Kangwanpongpan *et al.*, 2012. No explanation for such behavior is currently available, and this is left to future studies. Nevertheless, for all models, the fact that increasing the turbulence intensity decreases the WSGG error near the end of the optical path, where the intensities

Table 1. Differences between LBL and WSGG models for different levels of temperature fluctuation intensity

	C. *et al.*		D. *et al.*		K. *et al.*		Yin	
	Δ_{max}(%)	Δ_{avg}(%)	Δ_{max}(%)	Δ_{avg}(%)	Δ_{max}(%)	Δ_{avg}(%)	Δ_{max}(%)	Δ_{avg}(%)
$x/d = 30$:								
$TI = 0\,\%$	18.02	8.17	12.81	5.77	8.64	2.49	5.47	1.73
$TI = 50\,\%$	16.95	7.50	11.73	5.09	7.62	2.27	4.92	1.21
$TI = 100\,\%$	16.31	7.12	11.11	4.71	7.04	2.16	4.61	1.01
$TI = 150\,\%$	15.90	6.87	10.72	4.47	6.67	2.10	4.41	0.96
$x/d = 45$:								
$TI = 0\,\%$	17.18	8.36	9.76	4.14	9.92	2.94	6.18	1.73
$TI = 50\,\%$	16.22	7.55	8.85	3.38	8.89	2.54	5.43	1.90
$TI = 100\,\%$	15.48	6.96	8.19	2.85	8.15	2.31	4.89	2.04
$TI = 150\,\%$	14.94	6.55	7.71	2.49	7.62	2.20	5.49	2.17
$x/d = 60$:								
$TI = 0\,\%$	16.76	7.11	9.16	3.04	9.46	3.07	4.26	1.44
$TI = 50\,\%$	16.57	6.88	9.10	2.90	9.54	3.14	4.78	1.62
$TI = 100\,\%$	16.42	6.73	9.04	2.82	9.56	3.17	5.06	1.72
$TI = 150\,\%$	16.31	6.63	9.00	2.76	9.57	3.19	5.24	1.78

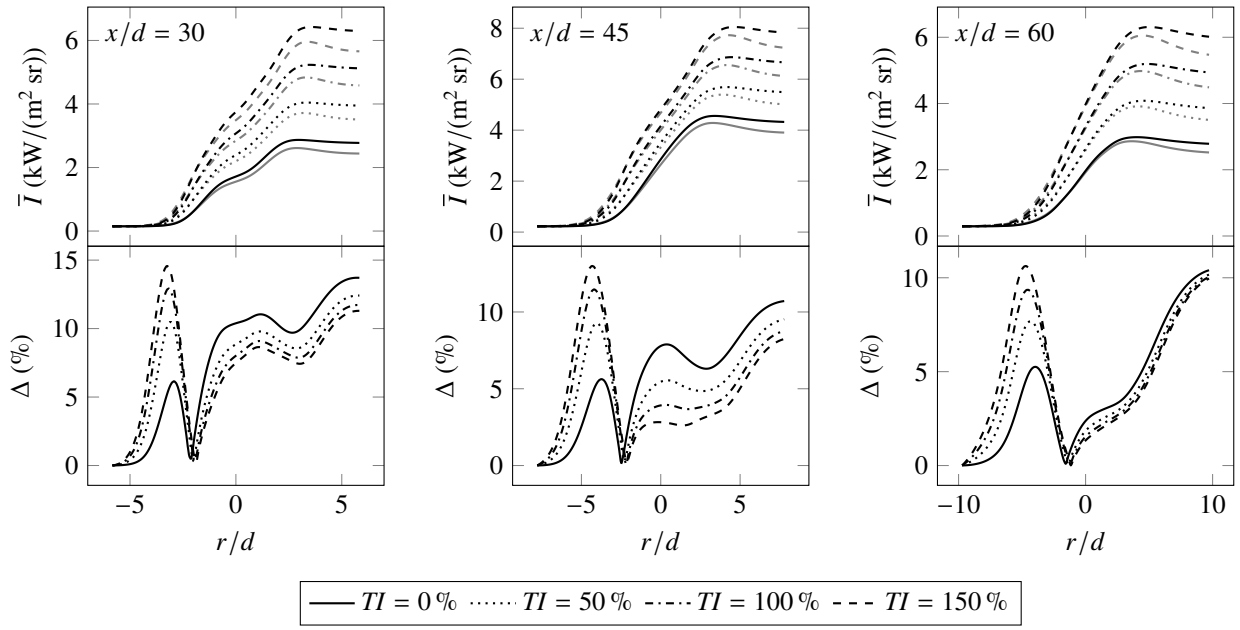

Figure 3. Mean radiation intensity computed by the LBL method (gray) and by the WSGG model of Dorigon *et al.*, 2013 (black) for different turbulence intensities, alongside the local errors of the latter.

themselves are larger, makes the TRI effect act to decrease the overall Δ, as remarked before.

Before concluding, it is important to note that the approach adopted in this paper for including the effect of turbulent fluctuations in the solution of the mean radiation field (which consisted of the OTFA and Snegirev's approximation for modeling absorption and emission TRI, respectively) involves a series of simplifications and has itself associated uncertainties. This is particularly true for the model for the mean emission, that is known to produce large errors in some cases, as discussed, for instance, in Fraga *et al.*, 2020. Other, more accurate (yet more complex and often more computationally intensive) TRI modeling approaches are available, such as probability density function-based methods and

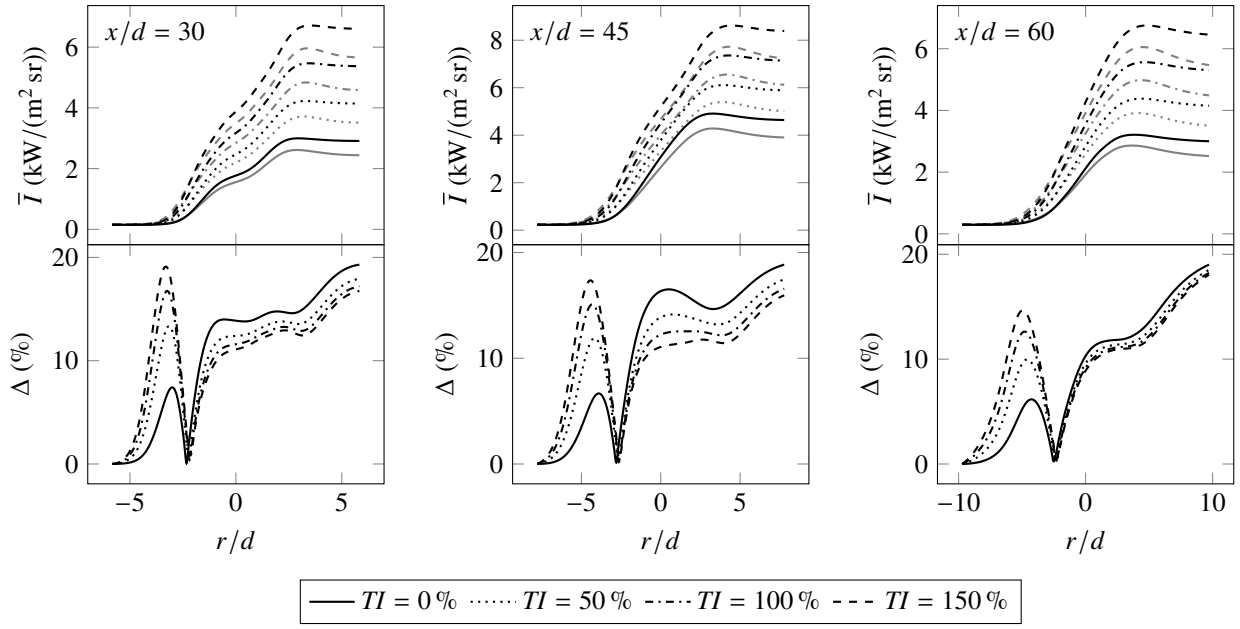

Figure 4. Mean radiation intensity computed by the LBL method (gray) and by the WSGG model of Cassol *et al.*, 2014 (black) for different turbulence intensities, alongside the local errors of the latter.

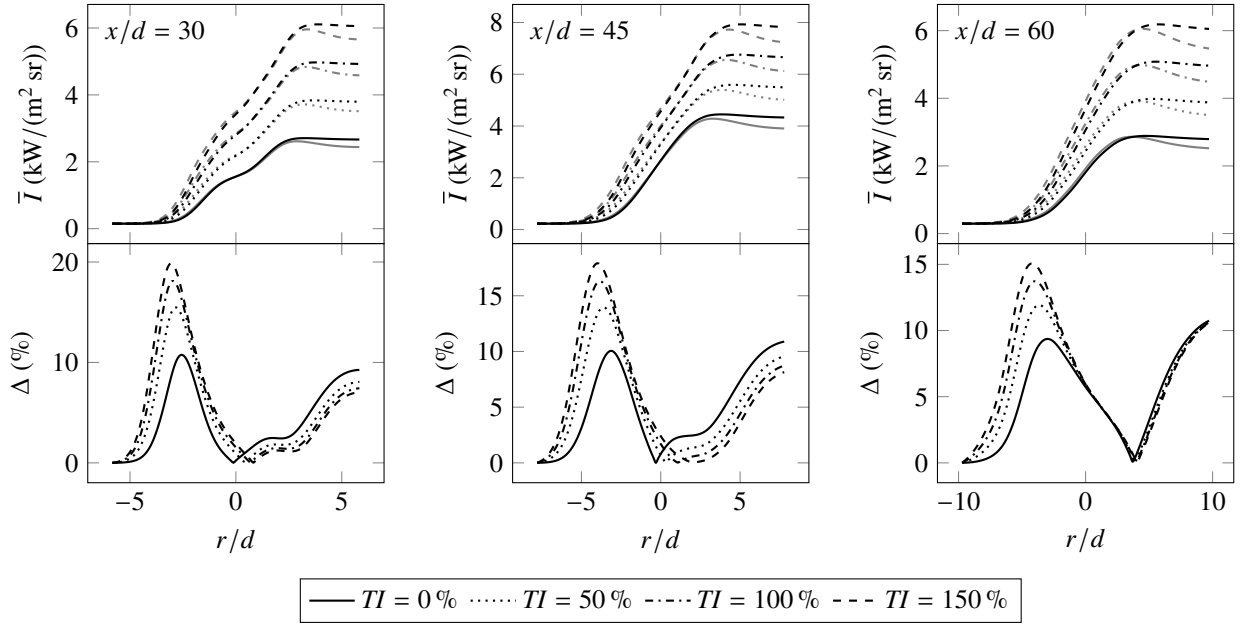

Figure 5. Mean radiation intensity computed by the LBL method (gray) and by the WSGG model of Kangwanpongpan *et al.*, 2012 (black) for different turbulence intensities, alongside the local errors of the latter.

solutions using stochastic series (Coelho, 2007), and should be tested in future studies.

5. CONCLUSIONS

This paper studied the effect of turbulent fluctuations on the accuracy of the weighted-sum-of-gray-gases model in estimating the mean radiation intensity. This was done by solving the time-averaged radiative transfer equation along three optical paths based on experimental data obtained for the Sandia flame D, using the optically thin fluctuation approximation to model the mean radiative absorption and the approximation developed by Snegirev, 2004, to treat the mean radiative emission. Four different formulations of the WSGG model were tested, and the reference to which they were compared was given by the line-by-line integration method.

Results showed that turbulent fluctuations greatly affect the radiation field, leading to a significant increase in the mean

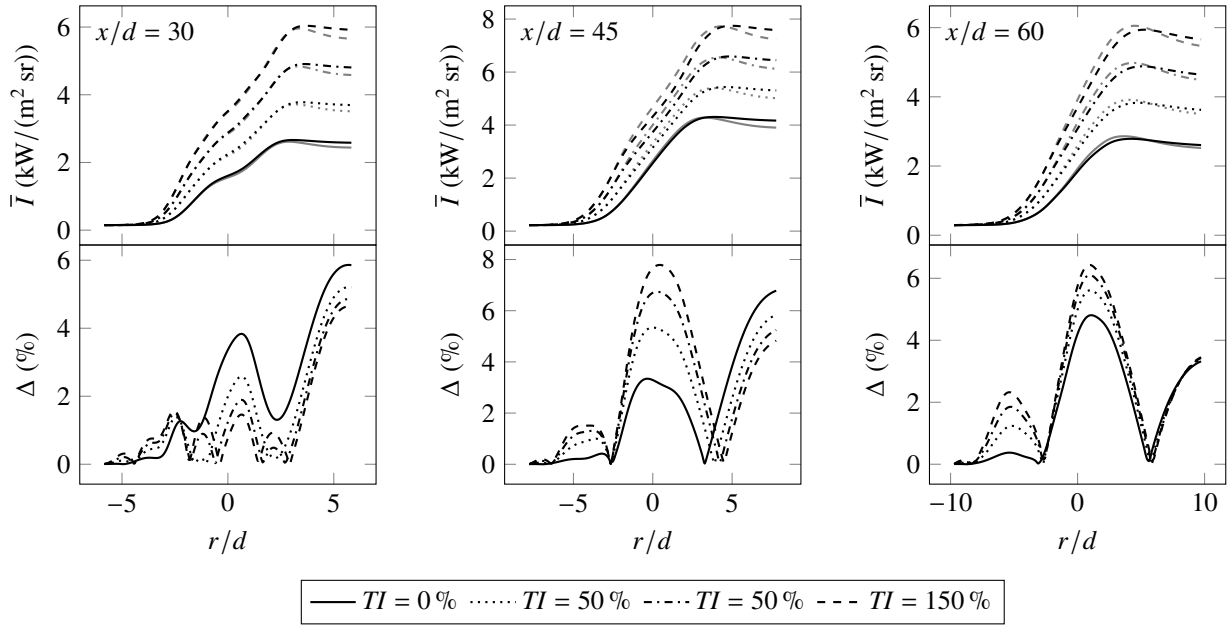

Figure 6. Mean radiation intensity computed by the LBL method (gray) and by the WSGG model of Yin, 2013 (black) for different turbulence intensities, alongside the local errors of the latter.

radiation intensity when they are considered. In general, the fluctuations act to decrease the errors of the WSGG model, although only slightly. This effect is also not uniform throughout the optical path—in fact, turbulent fluctuations tended to, in fact, increase the errors of the model at the beginning of the optical path, and it was only for the middle to the end of the path (where the radiation intensity is larger) that they had the opposite effect. Comparing the different WSGG formulation, the one by Yin, 2013, led to the most accurate results, followed by the one by Kangwanpongpan *et al.*, 2012, both with average errors of no more than 3 %.

6. ACKNOWLEDGEMENTS

Author BLZG thanks CAPES for a masters scholarship. Author GCF thanks CNPq for a doctoral scholarship. Author FHRF thanks CNPq for research grant 302686/2017-7.

7. REFERENCES

Barlow, R. and Frank, J., 1998. "Effects of turbulence on species mass fractions in methane/air jet flames". In *Symposium (International) on Combustion*. Elsevier, Vol. 27, pp. 1087–1095. doi:10.1016/s0082-0784(98)80510-9.

Bordbar, M.H., Wecel, G. and Hyppänen, T., 2014. "A line by line based weighted sum of gray gases model for inhomogeneous CO2-H2O mixture in oxy-fired combustion". *Combustion and Flame*, Vol. 161, No. 9, pp. 2435–2445. doi:10.1016/j.combustflame.2014.03.013.

Cassol, F., Brittes, R., França, F.H. and Ezekoye, O.A., 2014. "Application of the weighted-sum-of-gray-gases model for media composed of arbitrary concentrations of H_2O, CO_2 and soot". *International Journal of Heat and Mass Transfer*, Vol. 79, pp. 796–806. doi:10.1016/j.ijheatmasstransfer.2014.08.032.

Coelho, P.J., 2004. "Detailed numerical simulation of radiative transfer in a nonluminous turbulent jet diffusion flame". *Combustion and Flame*, Vol. 136, No. 4, pp. 481–492. doi:10.1016/j.combustflame.2003.12.003.

Coelho, P.J., 2007. "Numerical simulation of the interaction between turbulence and radiation in reactive flows". *Progress in Energy and Combustion Science*, Vol. 33, No. 4, pp. 311–383. doi:10.1016/j.pecs.2006.11.002.

Coelho, P.J., 2012. "Assessment of a presumed joint pdf for the simulation of turbulence-radiation interaction in turbulent reactive flows". *Applied Thermal Engineering*, Vol. 49, pp. 22–30. ISSN 13594311. doi:10.1016/j.applthermaleng.2011.06.032.

Coelho, P.J., Teerling, O.J. and Roekaerts, D., 2003. "Spectral radiative effects and turbulence/radiation interaction in a non-luminous turbulent jet diffusion flame". *Combustion and Flame*, Vol. 133, No. 1-2, pp. 75–91. doi:10.1016/S0010-2180(02)00542-4.

Dorigon, L.J., Duciak, G., Brittes, R., Cassol, F., Galarça, M. and França, F.H., 2013. "WSGG correlations based on HITEMP2010 for computation of thermal radiation in non-isothermal, non-homogeneous H_2O/CO_2 mixtures".

International Journal of Heat and Mass Transfer, Vol. 64, pp. 863–873. doi:10.1016/j.ijheatmasstransfer.2013.05.010.

Fraga, G.C., Coelho, P.J., Petry, A.P. and França, F.H.R., 2020. "Development and testing of a model for turbulence-radiation interaction effects on the radiative emission". *Journal of Quantitative Spectroscopy and Radiative Transfer*, Vol. 245, p. 106852. doi:10.1016/j.jqsrt.2020.106852. URL https://doi.org/10.1016%2Fj.jqsrt.2020.106852.

Gupta, A., Haworth, D.C. and Modest, M.F., 2013. "Turbulence-radiation interactions in large-eddy simulations of luminous and nonluminous nonpremixed flames". *Proceedings of the Combustion Institute*, Vol. 34, No. 1, pp. 1281–1288. ISSN 15407489. doi:10.1016/j.proci.2012.05.052.

Hall, R.J. and Vranos, A., 1994. "Efficient calculations of gas radiation from turbulent flames". *International Journal of Heat and Mass Transfer*, Vol. 37, No. 17, pp. 2745–2750. doi:10.1016/0017-9310(94)90391-3.

Howell, J.R., Mengüç, M.P. and Siegel, R., 2016. *Thermal Radiation Heat Transfer*. CRC press, 6th edition.

Kabashnikov, V. and Kmit, G., 1979. "Influence of turbulent fluctuations on thermal radiation". *Journal of Applied Spectroscopy*, Vol. 31, No. 2, pp. 963–967. doi:10.1007/bf00614832.

Kangwanpongpan, T., França, F.H., da Silva, R.C., Schneider, P.S. and Krautz, H.J., 2012. "New correlations for the weighted-sum-of-gray-gases model in oxy-fuel conditions based on HITEMP 2010 database". *International Journal of Heat and Mass Transfer*, Vol. 55, No. 25, pp. 7419–7433. doi:10.1016/j.ijheatmasstransfer.2012.07.032.

Krishnamoorthy, G., 2010. "A new weighted-sum-of-gray-gases model for CO_2-H_2O gas mixtures". *International Communications in Heat and Mass Transfer*, Vol. 37, No. 9, pp. 1182–1186. doi:doi.org/10.1016/j.icheatmasstransfer.2010.07.007.

Krishnamoorthy, G., 2012. "A comparison of angular discretization strategies for modeling radiative transfer in pool fire simulations". *Heat Transfer Engineering*, Vol. 33, No. 12, pp. 1040–1051. doi:10.1080/01457632.2012.659626.

Krishnamoorthy, G., Borodai, S., Rawat, R., Spinti, J. and Smith, P.J., 2005a. "Numerical modeling of radiative heat transfer in pool fire simulations". In *Heat Transfer, Part A*. ASME, Vol. 2005, pp. 327–337. ISBN 0-7918-4221-5. doi:10.1115/IMECE2005-81095.

Krishnamoorthy, G., Rawat, R. and Smith, P.J., 2005b. "Parallel computations of nongray radiative heat transfer". *Numerical Heat Transfer: Part B: Fundamentals*, Vol. 48, No. 2, pp. 191–211. doi:10.1080/10407790590963631.

Modest, M.F., 1991. "The weighted-sum-of-gray-gases model for arbitrary solution methods in radiative transfer". *Journal of Heat Transfer*, Vol. 113, No. 3, pp. 650–656. doi:10.1115/1.2910614.

Modest, M.F., 2013. *Radiative Heat Transfer*. Academic Press.

Modest, M.F. and Haworth, D.C., 2016. *Radiative Heat Transfer in Turbulent Combustion Systems: Theory and Applications*. Springer.

Pope, S.B., 2000. *Turbulent Flows*. Cambridge University Press, 1st edition.

Rothman, L.S., Gordon, I.E., Babikov, Y., Barbe, A., Benner, D.C., Bernath, P.F., Birk, M., Bizzocchi, L., Boudon, V., Brown, L.R. *et al.*, 2013. "The hitran2012 molecular spectroscopic database". *Journal of Quantitative Spectroscopy and Radiative Transfer*, Vol. 130, pp. 4–50. doi:10.1016/j.jqsrt.2013.07.002.

Rothman, L., Gordon, I., Barber, R., Dothe, H., Gamache, R., Goldman, A., Perevalov, V., Tashkun, S. and Tennyson, J., 2010. "Hitemp, the high-temperature molecular spectroscopic database". *Journal of Quantitative Spectroscopy and Radiative Transfer*, Vol. 111, No. 15, pp. 2139–2150. doi:10.1016/j.jqsrt.2010.05.001.

Snegirev, A.Y., 2004. "Statistical modeling of thermal radiation transfer in buoyant turbulent diffusion flames". *Combustion and Flame*, Vol. 136, No. 1, pp. 51–71. doi:10.1016/j.combustflame.2003.09.005.

TNF, 2020. "International workshop on measurement and computational of turbulent nonpremixed flames". URL https://www.sandia.gov/TNF/abstract.html.

Wilcox, D.C., 2006. *Turbulence Modeling for CFD*. DCW Industries, 3rd edition.

Yin, C., 2013. "Refined weighted sum of gray gases model for air-fuel combustion and its impacts". *Energy and Fuels*, Vol. 27, No. 10, pp. 6287–6294. doi:10.1021/ef401503r.

Yin, C., Johansen, L.C.R., Rosendahl, L.A. and Kær, S.K., 2010. "New weighted sum of gray gases model applicable to computational fluid dynamics (CFD) modeling of oxy-fuel combustion: Derivation, validation, and implementation". *Energy and Fuels*, Vol. 24, No. 12, pp. 6275–6282. doi:10.1021/ef101211p.

8. RESPONSIBILITY NOTICE

The authors are solely responsible for the printed material included in this paper.